

Coherent electron–hole correlations in quantum dots

Lars Jönsson,^{a)} Matthew M. Steiner, and John W. Wilkins

Department of Physics, Ohio State University, Columbus, Ohio 43210-1106

(Received 10 October 1996; accepted for publication 29 December 1996)

Using numerical time propagation of the electron–hole wave function, we demonstrate how various coherent correlation effects can be observed by laser excitation of a nanoscale semiconductor quantum dot. The lowest-lying states of an electron–hole pair, when appropriately excited by a laser pulse, give rise to charge oscillations that are manifested by beatings in the optical or intraband polarizations. A GaAs $5 \times 25 \times 25$ nm³ dot in the effective-mass approximation, including the screened Coulomb interaction between the electron and a heavy or light hole, is simulated. © 1997 American Institute of Physics. [S0003-6951(97)01909-8]

Semiconductor quantum dots with dimensions of the order of an exciton diameter (20 nm in GaAs) have unique optical properties due to the competition between confinement and correlation.¹ We demonstrate in this letter, by numerical time propagation including the screened Coulomb interaction, that coherent optical excitation of a few low-lying electron–hole-pair states gives rise to pronounced, measurable, correlation-induced beatings in the optical (interband) and intraband polarizations. These effects are important for two reasons: first, optical properties, e.g., the excitonic recombination rate, can be optically modulated, which may lead to new photonic applications; and second, the quantum dot is a new system, besides atoms, in which confined correlated electrons can be studied. The theoretical work on excitations in quantum dots was pioneered by Bryant, who applied configuration-interaction methods to obtain the correlated bound states.² Several geometries and materials have since been discussed,^{3–7} but the focus has been on unperturbed low-lying states, and on linear response. Our work addresses real-time dynamic correlation and coherence in quantum dots.

Experimentally, several types of nanoscale dots have been fabricated, and recent single-dot experiments have shown that the lowest-lying states often have sharp spectral features (50 μ eV),^{7,8} proving that true 0D structures with well-defined optical properties can be realized. It is, there-

fore, timely to discuss what new applications and physics to expect.

We use a prototypical GaAs ($\epsilon=13$, $E_{\text{gap}}=1.5$ eV, $m_e=0.07m_0$, $m_{\text{HH}}=0.5m_0$, $m_{\text{LH}}=0.08m_0$) quantum dot of size $5 \times 25 \times 25$ nm³ (denoted x , y , and z directions, respectively). Within the effective-mass approximation, we treat *either* an electron–heavy-hole *or* an electron–light-hole pair confined in the dot. We assume infinite potential walls and use sinusoidal basis orbitals, with $1 \times 4 \times 4$ orbitals for each particle giving convergence to within 1%. The Coulomb matrix elements are treated exactly within the orbital space. Two types of external fields are used: (i) optical laser pulses that interact via the optical dipole matrix elements; and (ii) far-infrared (FIR) laser fields that couple to the intraband dipole matrix elements in the z direction. Generally, an optical laser creates electron–hole pairs, while a FIR field polarizes the particles in the dot. Depending on symmetry and selection rules, we need, at most, 257 Slater determinants. The time propagation is performed with a Taylor-expansion method⁹ (typically, fifth order with a 0.5 fs time step).

We analyze the optical properties of the dot in terms of the time dependence of the optical and intraband polarizations. These observables are readily obtained numerically, since the operators involved are the same as those that couple to the external fields. However, it is not presently clear how to make the measurements experimentally. For quantum wells, time-resolved photoluminescence or four-wave mixing are commonly used. Being unable to mimic a particular experimental method, we assume that the polarizations can be measured directly or indirectly.

For the electron–heavy-hole system, the determinantal compositions of the four lowest-lying states are shown in Table I. [Notation: n is the quantum number of a sinusoidal orbital with $n-1$ nodes; a determinant is denoted

TABLE I. Determinantal composition of the four lowest-lying states of the electron–heavy-hole pair. The density distributions are shown in Fig. 1. The S and A stand for symmetrization and antisymmetrization of the y and z quantum numbers [e.g., $S(1,1;3,1)=[(1,1;3,1)+(1,1;1,3)]/\sqrt{2}$]. The first three determinants have even parity and the last one has odd parity in the z direction. States with odd parity in the y direction are not included since we consider electric fields only in the z direction. Interband electron–hole recombination occurs only in determinant (1,1;1,1). Determinants with occupation below 10% have been omitted.

Determinant ($n_{ey}, n_{ez}; n_{hy}, n_{hz}$)	State 1 1.734 eV	State 2 1.741 eV	State 3 1.750 eV	State 4 1.752 eV
(1,1;1,1)	0.86	0.00	0.37	0.00
$S(1,1;3,1)$	-0.39	0.00	0.82	0.00
$A(1,1;3,1)$	0.00	0.00	0.00	0.93
(1,1;1,2)	0.00	0.86	0.00	0.00

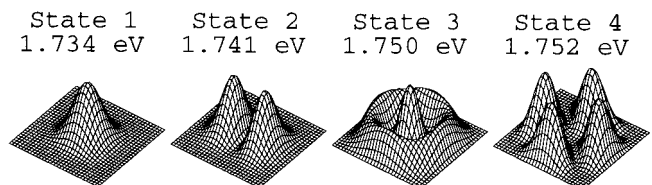


FIG. 1. Hole density distributions for the four lowest-lying states of the electron–heavy-hole pair. The determinantal compositions are given in Table I.

^{a)}Electronic mail: lars@pacific.mps.ohio-state.edu

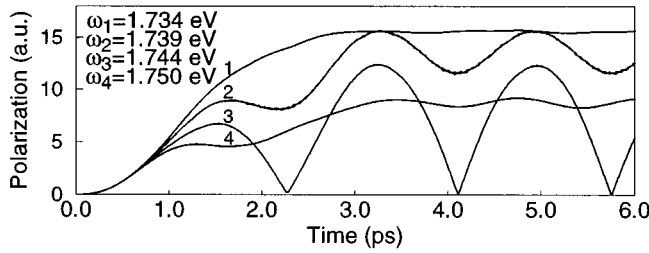


FIG. 2. Beatings in the optical polarization amplitude due to a coherent excitation of states 1 and 3 in Table I. For each of the four frequencies the electron–heavy-hole pair is created by a 3.3 ps laser pulse (maximum field = 6.7×10^{-6} a.u. = 3.4×10^6 V/m). In curve 3, where $\omega = 1.744$ eV, the electron–hole pair periodically reoccurs in a nonradiative state [i.e., no (1,1;1,1) component]. The density distributions at maximum and minimum optical polarization in curve 3 are shown in Fig. 3.

($n_{ey}, n_{ez}; n_{hy}, n_{hz}$); n_x is always 1 for both electrons and holes.] Due to the electron’s lighter mass, the states are all due to hole excitations. The corresponding hole charge distributions are shown in Fig. 1. Assuming an s -type conduction and p -type valence band, of the determinants shown, only the (1,1;1,1) determinant is radiative (the recombination selection rule is $n_{ey} = n_{hy}$ and $n_{ez} = n_{hz}$).¹⁰ This determinant is strongly coupled by the Coulomb interaction to the determinants (1,1;3,1) and (1,1;1,3). Consequently, states 1 and 3 can be optically excited; state 2 has odd parity in the z direction and couples to state 1 via a FIR field; and state 4 is a dark (optically decoupled) state.

With an initially empty dot, a laser pulse of a bandwidth close to the 16 meV energy separation of states 1 and 3 can create an electron–hole pair into a coherent superposition of the two states, which leads to beatings in the optical polarization (Fig. 2). The polarization is proportional to the time-dependent (1,1;1,1) coefficient. For a given bandwidth, there is an intermediate frequency at which the hole momentarily becomes nonradiative [no (1,1;1,1) component], the corresponding extrema of the oscillating charge distributions are shown in Fig. 3. The hole beats “radially” around the essentially immobile electron.

Another kind of charge oscillations that periodically puts the electron–hole pair into a nonradiative state is resonant Rabi oscillations between states 1 and 2 caused by a FIR field. Here, an optical pulse creates a pair in state 1, while a FIR laser drives the pair resonantly between state 1 and 2 with a Rabi frequency proportional to the field strength.¹¹ This driving leads to beatings both in the optical and the intraband polarizations (Figs. 4 and 5). The intraband polarization is strongest at equal mixing of the states, while the

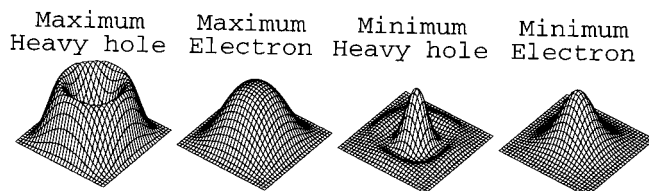


FIG. 3. Density distributions at maximum and minimum optical polarization for curve 3 in Fig. 2.

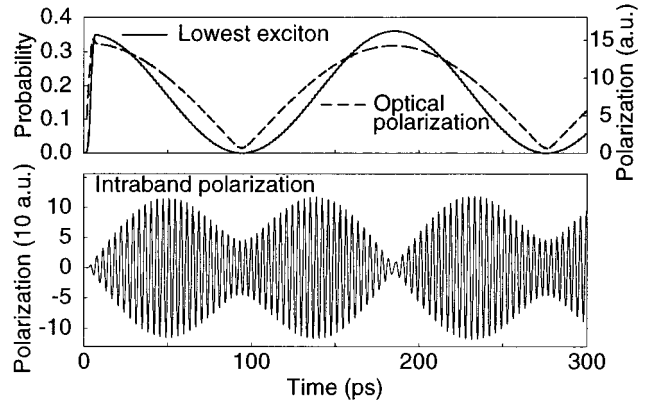


FIG. 4. Rabi oscillation between states 1 and 2 in Table I due to a resonant FIR field (maximum FIR field = 3.3×10^{-7} a.u.). Initially, the electron–hole pair is created in state 1 by a 7.2 ps laser pulse (maximum laser field = 3.3×10^{-6} a.u.). Since state 2 is nonradiative, the optical polarization amplitude (top, dashed curve) follows the beating in the population of state 1 (top, solid curve). The density distributions at maximum and minimum optical polarization are shown in Fig. 5. Maximum intraband polarization (bottom curve) is obtained with equal population of both states, while each state alone is unpolarized.

pure states are unpolarized. While for a two-level system this is strictly true, in our case the higher-lying states dynamically couple to state 2, leading to an imperfect minimum.

In contrast to the heavy-hole system, where the electron is passive, similar experiments in the light-hole system involve true dynamic correlations. Table II shows the composition of the four lowest-lying electron–light-hole states of even parity (see Fig. 6). Note in states 2 and 4 the coupling between the radiative (2,1;2,1)- and nonradiative (3,1;1,1)-type determinants, which coupling is a pure correlation effect since both the electron and the hole quantum numbers change. States 2 and 4 can be coherently excited by a laser pulse of about 12 meV bandwidth (state 3 is dark). This leads to a beating in the optical polarization (Fig. 7) that is a pure correlation effect. The charge oscillations are now more subtle, but again the electron–hole pair oscillates between a radiative and a nonradiative state.

In conclusion, we have shown for a prototypical quantum dot that strong correlation effects can be observed by relatively simple coherent excitations of a few low-lying states. An electron–hole pair can be made to oscillate in and out of a nonradiative state, which makes the effect observable in the first place, but also opens the possibility of controlled optical modulations of the optical properties.

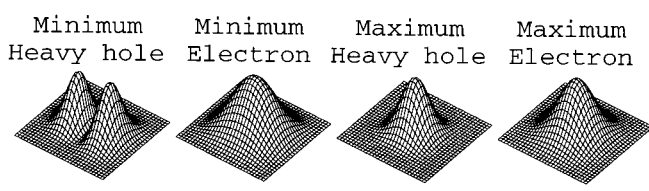


FIG. 5. Density distributions at maximum and minimum optical polarization for the situation in Fig. 4.

TABLE II. Determinantal composition of the four lowest-lying even-parity states of the electron–light-hole pair. See Table I for notational details. The density distributions are shown in Fig. 6.

Determinant ($n_{ey}, n_{ez}; n_{hy}, n_{hz}$)	State 1 1.909 eV	State 2 1.957 eV	State 3 1.960 eV	State 4 1.969 eV
(1,1;1,1)	0.98	-0.10	0.00	0.18
S(2,1;2,1)	0.16	0.91	0.00	-0.37
S(3,1;1,1)	-0.08	0.23	0.00	0.41
S(1,1;3,1)	-0.09	0.31	0.00	0.79
A(2,1;2,1)	0.00	0.00	0.89	0.00

Clearly, inhomogeneous broadening and fluctuations in the laser pulses will smear the perfect minima of the numerical simulations. However, since the ideal dot has perfect minima there is hope that a realistic ensemble of dots will have observable beatings. It is also important that only a few low-lying states are involved, since they have been found experimentally to have sharp spectral features.

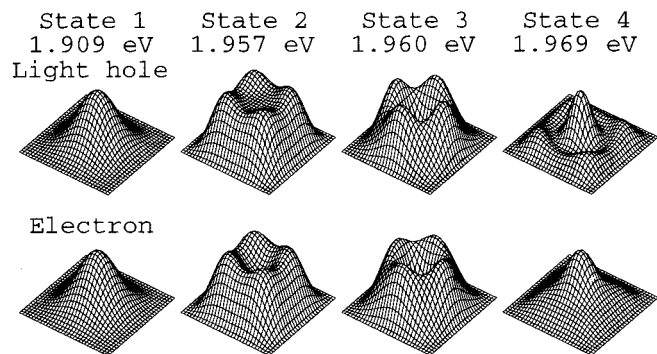


FIG. 6. Density distributions for the four lowest-lying even-parity states of the electron–light-hole pair. The determinantal compositions are given in Table II. States 1 and 4 roughly correspond to states 1 and 3 of the electron–heavy-hole pair (Fig. 1).

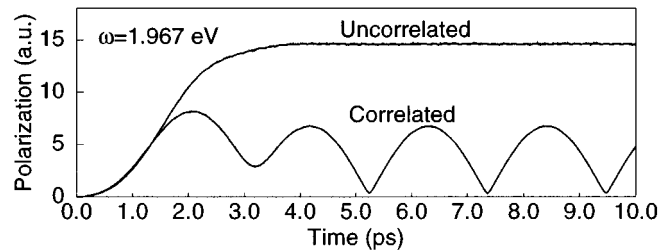


FIG. 7. Coherent beating in the optical polarization amplitude due to a superposition of states 2 and 4 in Table II. The beating is a pure correlation effect. The electron–hole pair is created by a 4.3 ps laser pulse (maximum field= 5.0×10^{-6} a.u.) at $\omega=1.967$ eV, which frequency gives the lowest minimum in the correlated case.

This work was supported by the Office of Naval Research, by the Department of Energy–Basic Energy Sciences, Division of Materials Science, and by the Ohio Supercomputer Center.

- ¹See, for example, H. Gotoh, H. Ando, and H. Kanbe, *Appl. Phys. Lett.* **68**, 2132 (1996); J. M. Gérard, O. Cabrol, and B. Sermage, *ibid.* **68**, 3123 (1996).
- ²G. W. Bryant, *Phys. Rev. Lett.* **59**, 1140 (1987).
- ³G. W. Bryant, *Phys. Rev. B* **41**, 1243 (1990); **47**, 1683 (1993); **48**, 8024 (1993).
- ⁴Y. Z. Hu, M. Lindberg, and S. W. Koch, *Phys. Rev. B* **42**, 1713 (1990).
- ⁵R. Romestain and G. Fishman, *Phys. Rev. B* **49**, 1774 (1994).
- ⁶M. Grundmann, O. Stier, and D. Bimberg, *Phys. Rev. B* **52**, 11 969 (1995).
- ⁷M. Grundmann, N. N. Ledentsov, O. Stier, D. Bimberg, V. M. Ustinov, P. S. Kop'ev, and Zh. I. Alferov, *Appl. Phys. Lett.* **68**, 979 (1996), and references therein.
- ⁸D. Gammon, E. S. Snow, B. V. Shanabrook, D. S. Katzer, and D. Park, *Phys. Rev. Lett.* **76**, 3005 (1996); *Science* **273**, 87 (1996).
- ⁹Th. Mercouris, Y. Komninos, S. Dionissopoulou, and C. A. Nicolaides, *Phys. Rev. A* **50**, 4109 (1994).
- ¹⁰G. Bastard, *Wave Mechanics Applied to Semiconductor Heterostructures* (Halsted Press, Wiley, New York, 1988), p. 246.
- ¹¹L. Allen and J. H. Eberly, *Optical Resonance and Two-Level Atoms* (Dover, New York, 1987), p. 56.